Biological Cybernetics (2019) 113:149–159
https://doi.org/10.1007/s00422-018-0783-9

Biological Cybernetics

ORIGINAL ARTICLE

An optimal control approach for blood pressure regulation during head-up tilt

Nakeya D. Williams[1] · Jesper Mehlsen[2] · Hien T. Tran[3] · Mette S. Olufsen[3]

Received: 20 August 2018 / Accepted: 29 September 2018 / Published online: 30 October 2018

Abstract

This paper presents an optimal control approach to modeling effects of cardiovascular regulation during head-up tilt (HUT). Many patients who suffer from dizziness or light-headedness are administered a head-up tilt test to explore potential deficits within the autonomic control system, which maintains the cardiovascular system at homeostasis. This system is complex and difficult to study in vivo, and thus we propose to use mathematical modeling to achieve a better understanding of cardiovascular regulation during HUT. In particular, we show the feasibility of using optimal control theory to compute physiological control variables, vascular resistance and cardiac contractility, quantities that cannot be measured directly, but which are useful to assess the state of the cardiovascular system. A non-pulsatile lumped parameter model together with pseudo- and clinical data are utilized in the optimal control problem formulation. Results show that the optimal control approach can predict time-varying quantities regulated by the cardiovascular control system. Our results compare favorable to our previous study using a piecewise linear spline approach, less *a priori* knowledge is needed, and results were obtained at a significantly lower computational cost.

Keywords Cardiovascular dynamics modeling · Head-up tilt · Non-pulsatile model · Orthostatic intolerance · Optimal control

1 Introduction

The short-term response to orthostatic stress involves complex interaction among control mechanisms engaged to keep the cardiovascular system at homeostasis. The most notable control mechanism, the baroreceptor reflex, operates by changing cardiovascular efferents in response to changes in blood pressure (BP). The HUT test is often used to assess patients ability to regulate blood pressure, in particular for patients who suffer from frequent episodes of syncope, light-headedness, or dizziness (Miller and Kruse 2005). During the HUT test, the patient first rests on a tilt-table in supine position. After steady values for pressure and heart rate (HR) have been established, the table is tilted to an angle of 60 degrees. Upon tilting, gravity pools approximately 500–1000 ml of blood in the lower extremities reducing venous return, which induces a reduction in cardiac filling, pressure and volume (Lanier et al. 2011; Rowell 2004). In response, blood pressure in the upper body is decreased, while blood pressure in the lower body is increased. For healthy people, baroreceptors located in the carotid sinuses sense the drop in blood pressure causing sympathetic activation and parasympathetic withdrawal, which in turn lead to an increase in heart rate, cardiac contractility, and vascular resistance, while vascular compliance is decreased (Robertson et al. 2004). For patients with autonomic dysfunction, e.g. orthostatic hypotension, postural change is associated with severe risks including dizziness, loss of balance lead-

Communicated by Pablo A. Iglesias.

This article belongs to the Special Issue on *Control Theory in Biology and Medicine*. It derived from a workshop at the Mathematical Biosciences Institute, Ohio State University, Columbus, OH, USA.

✉ Mette S. Olufsen
msolufse@ncsu.edu

Nakeya D. Williams
nakeya.williams@usma.edu

Jesper Mehlsen
Jesper.Mehlsen@region.dk

Hien T. Tran
tran@ncsu.edu

[1] United States Military Academy, West Point, New York, USA

[2] Bispebjerg and Frederiksberg Hospital, Frederiksberg, Denmark

[3] NC State University, Raleigh, NC, USA

ing to falls, and reflex mediated syncope, in particular, for the elderly and for patients with hypertension and diabetes. The underlying pathophysiology associated with autonomic dysfunction is not well understood, making it difficult to derive a model predicting the system failure. To remedy this problem, this study shows how optimal control theory can be used to predict autonomic regulation during HUT.

Some previous biophysical applications have considered optimal control methodologies, in disease modeling, e.g. to design treatment strategies for HIV and cancer patients (David 2007; Pillis and Radunskaya 2003; Neilan and Lenhart 2010; Zarei et al. 2010), in cardiac physiology to terminate reentry waves in cardiac electrophysiology (Nagaiah et al. 2013) or to control the heart pump function (Shoucri 1991). A few studies have used optimal control theory for predicting physiological markers within the cardiovascular and respiratory systems (Batzel et al. 2005; Fink et al. 2004; Kappel et al. 2007; Mutsaers et al. 2007). These studies employed optimal control theory to study the effects of congestive heart failure on the cardiovascular and respiratory control systems. In this paper, we propose to use optimal control theory as a tool to predict how the baroreflex system modulate vascular resistance and cardiac contractility during HUT.

Previous efforts to regulate vascular resistance and cardiac contractility included parametrizing these variables using piecewise linear splines in the context of a nonlinear least-squares problem formulation (Williams et al. 2014) and nonlinear filtering (Matzuka et al. 2015). The spline method proved to be computationally expensive, and it requires *a priori* knowledge of the system for placement of the nodes for the splines. The spread of the nodes were manually specified in the model. During HUT, where dynamics change rapidly, significantly more points were needed to increase model fidelity. It should be noted that as more points are added to parametrize the control variables, the dimensionality of the optimization problem would also increase. Nonlinear filtering provides a sequential approach for online joint estimation of both state variables and parameters and the possibility of tracking parameters (e.g., vascular resistance and cardiac contractility) whose values drift over time. Implementation of a filter requires knowledge of the model noise and measurement noise. How to properly assign these error variances is an ongoing area of research in filtering.

The goal here is to use an optimal control methodology to predict dynamics of quantities modulated by the baroreflex system (vascular resistance and cardiac contractility) in individual patients. This approach has potential to allow clinicians to use a model based approach to assess cardiovascular regulation in individual patients, revealing how quantities that cannot be measured change in time. A promising approach for approximating the solution to the optimal control problem is the direct transcription method (Engelsone 2006). This method reformulates the continuous optimal control problem as a discrete optimization problem, an approach often referred to as "discretize then optimize". In this study, the optimal control problem is solved using a General Pseudo-Spectral Optimal Control Software (GPOPS), a MATLAB based optimal control software that uses an adaptive Radau pseudo-spectral method to transcribe the optimal control problem to a nonlinear programming problem (NLP) (Rao et al. 2011). The NLP is then solved using either the NLP solver SNOPT or IPOPT. Results from GPOPS are subsequently compared with those obtained using the piecewise linear spline parameterization (Williams et al. 2014).

2 Methods

This section first describes the cardiovascular model, followed by a description of data, and the optimal control method used for prediction of quantities regulated by the baroreflex system.

2.1 Cardiovascular model

Systemic blood flow, volume, and pressure changes in response to HUT are predicted using the non-pulsatile lumped parameter model depicted in Fig. 1. The model includes compartments representing arteries and veins in the upper and lower body as well as a compartment representing the heart.

For each compartment, a pressure–volume relation is given by

$$V_{\mathrm{i}} - V_{\mathrm{un}} = C_{\mathrm{i}}(p_{\mathrm{i}} - p_{\mathrm{ext}}), \tag{1}$$

where V_{i} (ml) is the compartment volume, V_{un} (ml) the unstressed volume, C_{i} (ml/mmHg) the compliance, p_{i} (mmHg) the instantaneous blood pressure, and p_{ext} (mmHg) (assumed constant) the pressure in the surrounding tissue. Here, the subscript i denotes the ith compartment. The change in volume within a compartment is computed as

$$\frac{\mathrm{d}V_{\mathrm{i}}}{\mathrm{d}t} = q_{\mathrm{in}} - q_{\mathrm{out}}, \tag{2}$$

where q (ml/s) is the volumetric flow. Using a linear relationship analogous to Ohm's law, the volumetric flow q (ml/s) between compartments can be computed as

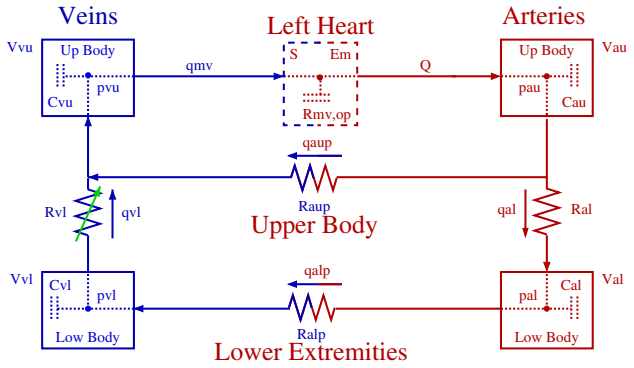

Fig. 1 Non-pulsatile compartment model used for predicting HUT dynamics. Each compartment is associated with a blood pressure p (mmHg), volume V (ml), and compliance C (ml/mmHg), while flow q (ml/s) is determined between compartments. The compartments represent the upper body arteries (subscript au), lower body arteries (subscript al), upper body veins (subscript vu), lower body veins (subscript vl), and the left heart (subscript lh). Resistances R (mmHg s/ml) are placed between compartments: R_{al} denotes the resistance between arteries in the upper and lower body, R_{aup} and R_{alp} denote resistances between arteries and veins in the upper and lower body, respectively. The left heart dynamics is described using parameters representing the contractility (S), minimum elastance (E_{m}), and open mitral valve ($R_{\mathrm{mv,op}}$) of the heart. Finally, the resistance between the lower and upper body veins R_{vl} is modeled as pressure dependent to prevent retrograde flow into the lower body during HUT

$$q = \frac{p_{\mathrm{in}} - p_{\mathrm{out}}}{R}, \tag{3}$$

where p_{in} and p_{out} are the pressure on either side of the resistor R (mmHg s/ml). Differentiating (1), using (2), and inserting (3) allows us to obtain a system of differential equations in blood pressure of the form

$$\frac{dp_i}{\mathrm{d}t} = \frac{1}{C_i}\frac{\mathrm{d}V_i}{\mathrm{d}t} = \frac{1}{C_i}\left(\frac{p_{i-1} - p_i}{R_{i-1}} - \frac{p_{\mathrm{i}} - p_{i+1}}{R_{\mathrm{i}}}\right),$$

where i refers to the compartment in which the pressure p_i is computed, while $i - 1$ and $i + 1$ refer to the two neighboring compartments. R_{i-1} refers to the resistance between compartments $i - 1$ and i, while R_i refers to the resistance between compartments i and $i + 1$. The latter equation is valid since we assume that C_{i} (ml/mmHg) is constant.

The non-pulsatile heart model is adapted from work by Batzel et al. (2007), which followed ideas originally proposed by Grodins (1959). This model predicts cardiac output Q (the flow out of the left ventricle) as a function of venous filling pressure p_{pv} and heart rate H. The model is derived by averaging dynamics during cardiac filling (when the mitral valve is open) and ejection (when the aortic valve is open).

Cardiac filling is modeled assuming that the inflow into the ventricle depends on the difference between the filling pressure and the left ventricle pressure using an expression analogous to (3) of the form

$$\dot{V}_{\mathrm{lh}}(t) = \frac{1}{R_{\mathrm{mv,op}}}(p_{\mathrm{pv}}(t) - p_{\mathrm{lh}}(t)), \tag{4}$$

where V_{lh} is the ventricular volume at time t after the filling process has started, p_{lh} is the ventricular pressure, p_{pv} is the venous filling pressure, and $R_{\mathrm{mv,op}}$ is the ventricular resistance to flow when the mitral valve is open.

For the relaxed ventricle, a similar volume pressure relation, similar to (1) is given by

$$p_{\mathrm{lh}}(t) = E_{\mathrm{m}}(V_{\mathrm{lh}}(t) - V_{\mathrm{un}}), \tag{5}$$

where V_{un} denotes the unstressed volume of the relaxed ventricle and E_{m} denotes the minimum elastance of the left heart. The initial value for (4) is given by $V_{\mathrm{lh}}(0) = V_{\mathrm{ES}}$, where V_{ES} denotes the end-systolic volume. Substituting (5) into (4), then solving the differential equation in (4) at $t = t_d$, the time of end-diastole onset, we obtain

$$V_{\mathrm{ED}} = kV_{\mathrm{ES}} + a\left(\frac{p_{\mathrm{pv}}}{E_{\mathrm{m}}} + V_{\mathrm{un}}\right), \tag{6}$$

where $k = \exp(-t_d E_{\mathrm{m}}/R_{\mathrm{lh}})$, $a = 1 - k$. In addition, $t_d = T - T_M$ denotes the time at onset of end-diastole and T_M denotes the end-systole onset time.

The work presented in Batzel et al. (2007) predicted cardiac output from both the systemic and pulmonary circulation. However, this study only includes the left ventricle of the systemic circulation, and consequently predicts cardiac output as a function of systemic venous pressure p_{vu}.

Cardiac output (Q) is defined as the product of heart rate and stroke volume, that is,

$$Q = HV_{\mathrm{str}}, \tag{7}$$

where V_{str} is the stroke volume, the volume of blood ejected during one stroke, and H is the heart rate. The stroke volume is given by

$$V_{\mathrm{str}} = V_{\mathrm{ED}} - V_{\mathrm{ES}}, \tag{8}$$

where V_{ED} is the end-diastolic volume (predicted using (6) and V_{ES} is the end-systolic volume.

While it was fairly straightforward to predict V_{ED}, additional assumptions are needed to predict V_{ES}. It is difficult to derive an expression for V_{ES}, yet this term can be eliminated assuming cardiac ejection can be predicted as a function of arterial and venous pressures acting on the ventricle. This idea is incorporated in the so-called Frank–Starling mechanism (Burton 1972), which suggests that stroke volume increases proportionally to the end-diastolic volume, when all other factors remain constant. Consequently, increased filling of the ventricle during diastole causes an increased

contraction force during the following systole. This is modeled as

$$V_{\text{str}} = \frac{S}{p_a}(V_{\text{ED}} - V_{\text{un}}), \tag{9}$$

where p_a is the arterial pressure against which the ventricle has to eject (the after load) and S denotes the contractility of the left ventricle. In this study, $p_a = 0.98 p_{\text{au}}$, the blood pressure of the arterial upper body.

The previous expressions are used to predict the cardiac output Q as a function of blood pressure. Equations (6), (8), and (9) constitute a system of equations for V_{ED}, V_{ES}, and V_{str} of the form

$$V_{\text{ED}} = \frac{p_{\text{pv}}}{E_{\text{m}}} + V_{\text{un}} - \frac{k p_{\text{pv}} S}{E_{\text{m}}(a p_{\text{au}} + kS)}, \tag{10}$$

$$V_{\text{ES}} = \frac{p_{\text{pv}}}{E_{\text{m}}} + V_{\text{un}} - \frac{p_{\text{pv}} S}{E_{\text{m}}((1-k) p_{\text{au}} + kS)}, \tag{11}$$

$$V_{\text{str}} = V_{\text{ED}} - V_{\text{ES}} = \frac{(1-k) p_{\text{pv}} S}{E_{\text{m}}((1-k) p_{\text{au}} + kS)}. \tag{12}$$

Recall that our model does not include both the systemic and pulmonary circuits, and thus we do not have a component for venous filling pressure p_{pv}. The incoming pressure into the ventricle in this model is the upper body venous pressure p_{vu}. Generally, $p_{\text{pv}} > p_{\text{vu}}$ (Smith and Kampine 1990). To compensate for the difference between the two venous pressures, p_{vu} is multiplied by a constant factor c, $p_{\text{pv}} = c p_{\text{vu}}$. Subsequently, combining (7) and (12) gives the cardiac output out of the ventricle

$$Q = H \frac{(1-k) c p_{\text{v}} S}{E_{\text{m}}((1-k) p_{\text{a}} + kS)}. \tag{13}$$

Using these relations, the differential equations can be written as

$$\frac{dp_{\text{au}}}{\text{d}t} = \left(Q - q_{\text{al}} - q_{\text{aup}}\right)/C_{\text{au}} \tag{14}$$

$$\frac{dp_{\text{al}}}{\text{d}t} = \left(q_{\text{al}} - q_{\text{alp}}\right)/C_{\text{al}} \tag{15}$$

$$\frac{dp_{\text{vl}}}{\text{d}t} = \left(q_{\text{alp}} - q_{\text{vl}}\right)/C_{\text{vl}} \tag{16}$$

$$\frac{dp_{\text{vu}}}{\text{d}t} = \left(q_{\text{aup}} + q_{\text{vl}} - Q\right)/C_{\text{vu}}, \tag{17}$$

where

$$q_{\text{aup}} = \frac{p_{\text{au}} - p_{\text{vu}}}{R_{\text{aup}}}$$

$$q_{\text{al}} = \frac{p_{\text{au}} - p_{\text{al}}}{R_{\text{al}}}$$

$$q_{\text{alp}} = \frac{p_{\text{al}} - p_{\text{vl}}}{R_{\text{alp}}}$$

$$q_{\text{vl}} = \frac{p_{\text{vl}} - p_{\text{vu}}}{R_{\text{vl}}}.$$

2.2 Data

Beat-to-beat blood pressure was measured using a Finapres device (Finapres Medical Systems, B.V.), and heart rate was measured using standard precordial leads. Data were collected at the Coordinating Research Centre at Bispebjerg and Frederiksberg Hospital, Copenhagen, Denmark, from five healthy young male volunteers age 30 ± 4 who were fit and had no known heart or vascular diseases. The subjects gave informed consent to participate in the study, which was approved by the local internal review board at Bispebjerg and Frederiksberg Hospital, Denmark. After resting for 10 minutes in supine position, the subjects were tilted to an angle of 60 degrees at a speed of 15 degrees per second measured by way of an electronic marker. The subjects remained tilted for five minutes and were then returned to supine position at the same tilt speed. For the model based analysis, we extracted a 180 second segment recorded during HUT. (See Fig. 2 left.) As discussed in our previous study (Williams et al. 2014), to accurately predict vascular resistance and cardiac contractility, cardiac output is essential. However, since cardiac output is not measured, we use pseudo-cardiac output data (Fig. 2 right) obtained from averaging estimates from the pulsatile model developed in our previous study (Williams et al. 2014). For future studies, we recommend to couple blood pressure and heart rate measurements with measurements of cardiac output, e.g. using echocardiography.

In addition to utilizing clinical data to validate the model, we also use pseudo-data for model validation. These pseudo-data are extracted from our previous work (Williams et al. 2014) using a pulsatile model to predict resting heart rate and blood pressure. More explanation of the pseudo-data and how it is used will be discussed in Sect. 3.1.

2.3 Optimal control formulation

We formulate the problem of predicting levels of vascular resistance and cardiac contractility, modulated by the baroreflex system during HUT, as a tracking problem. To this end, we define the objective functional

$$J = \int_{t_0}^{t_f} \left\{ 10^2 \left[\left(\frac{p_{\text{au}}^m - p_{\text{au}}^d}{p_{\text{au}}^d} \right)^2 + \left(\frac{p_{\text{vu}}^m - p_{\text{vu}}^d}{p_{\text{vu}}^d} \right)^2 + \left(\frac{p_{\text{al}}^m - p_{\text{al}}^d)}{p_{\text{al}}^d} \right)^2 + \left(\frac{p_{\text{vl}}^m - p_{\text{vl}}^d)}{p_v l^d} \right)^2 \right.$$

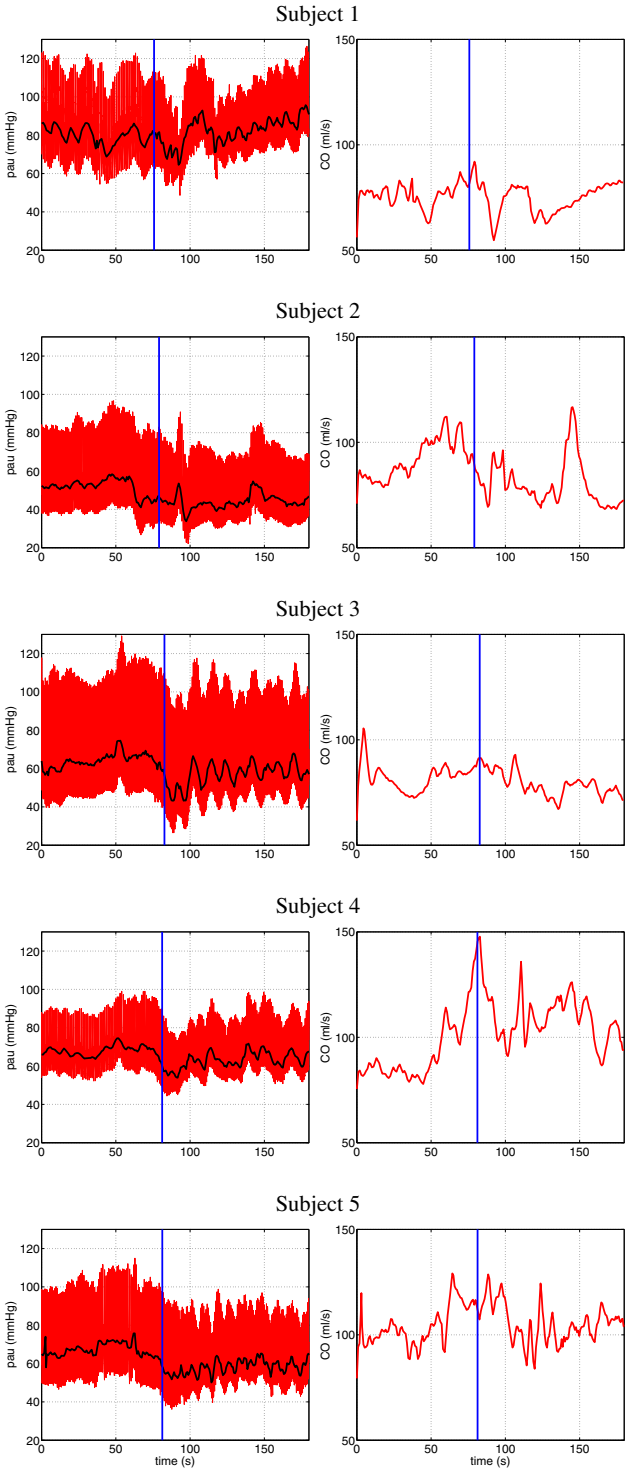

Fig. 2 Upper body arterial blood pressure (left) and cardiac output (right) data from five healthy young male subjects during HUT. The dark blue line indicates the onset of HUT, and the black curve denotes the mean blood pressure (averaged over each cardiac cycle)

$$+\left(\frac{\mathrm{CO}^m-\mathrm{CO}^d}{\mathrm{CO}^d}\right)^2 + \left(\frac{V^m_{tot}-V^d_{tot}}{V^d_{tot}}\right)^2\Bigg] + R^2_{\mathrm{aup}} + E^2_{\mathrm{m}}\Bigg\}\,\mathrm{d}t, \tag{18}$$

where superscript d refers to the pseudo-data and m refers to the non-pulsatile model predicted quantities. In particular, the pseudo-data p^d_{au}, p^d_{vu}, p^d_{al}, p^d_{vl}, and CO^d denote the mean of pressures and cardiac output from the pulsatile model predictions in Williams et al. (2014). They are concatenated together from each cardiac cycle to form the tracking data. The control variables are the upper body peripheral resistance R_{aup} and the minimum elastance E_{m}. The weights in (18) have been determined *a priori* through a series of numerical experiments. The optimal tracking control problem is to find the control $u(t) = (R_{\mathrm{aup}}(t), E_{\mathrm{m}}(t))$ minimizing the objective functional (18) subject to the state Eqs. (14–17) with some initial conditions.

We note that our mathematical model for the cardiovascular system dynamics (14–17) is nonlinear. In general, there are two approaches for the numerical solution of optimal control problems. Indirect methods are based on the calculus of variations and Pontryagin's principle to determine the first-order necessary conditions for optimality (Betts 1998; Stryk and von and Burlirsch 1992). On the other hand, in direct methods, the continuous state, control, and objective functional are approximated and the optimal control problem is transcribed into a finite-dimensional nonlinear programming problem (NLP). The NLP is solved using well-developed algorithms and software (Murray et al. 2002; Saunders et al. 1986). The direct methods have the advantage that the optimality necessary conditions do not need to be derived. On the other hand, direct methods require more work to verify optimality and they, in general, do not provide knowledge of the co-state variables. Among many established direct methods is the collocation method where both the state and control variables are parametrized by a set of basis functions and a set of differential algebraic constraints are enforced at a finite number of collocation points. The collocation based direct methods have been implemented in a number of computer softwares including GPOPS (Rao et al. 2010), which we employed in our numerical solution for the optimal tracking problem. GPOPS (General Pseudo-spectral Optimal Control Software) solves multiphase optimal control problems using the Radau Pseudo-spectral Method (RPM). The RPM is an orthogonal collocation method where the collocation points are the Legendre Gauss Radau points (Rao et al. 2011). One of the nice features of the RPM is that it has been shown to converge exponentially fast for problems with smooth solutions.

Table 1 Steady-state bounds for GPOPS

Quantity	Start lower bound	During lower bound	End lower bound	Start upper bound	During upper bound	End upper bound
p_{au}	71.1	68	68	71.1	80	80
p_{vu}	2.6	2	2	2.6	3	3
p_{al}	69.7	68	68	69.7	80	80
p_{vl}	2.9	2.7	2.7	2.9	3	3
R_{aup}	0.75	–	0.75	0.95	–	0.95
E_m	0.005	–	0.005	0.02	–	0.02

Table 2 Tilt bounds for GPOPS

Quantity	Start lower bound	During lower bound	End lower bound	Start upper bound	During upper bound	End upper bound
p_{au}	67.8	50	50	67.8	100	100
p_{vu}	2.6	0.3	0.3	2.6	3.5	3.5
p_{al}	66.4	50	50	66.4	115	115
p_{vl}	2.9	1	1	2.9	25	25
R_{aup}	0.2	–	0.2	1.1	–	1.1
E_m	0.005	–	0.005	0.017	–	0.017

GPOPS requires the user to specify boundary conditions on the state and control variables. For our problem, these values, which were chosen based on results from previous work (Williams et al. 2013; Williams et al. 2014), are given in Table 1 and Table 2 for the steady-state and tilt portions of the simulation, respectively.

It should also be noted that the control variables change on a slower timescale when compared to the timescale of the pulsatile model, hence making it infeasible to find simultaneous solutions for the state equations and the control variables. Furthermore, the differences in timescales for the state dynamics and the control variables stem from the fact that the controls try to resolve dynamics within a single beat rather than between beats as in the pulsatile model. As a result, with the pulsatile model, an abundance of collocation points are needed to solve the optimal control problem effectively. The more collocation points used, the longer the simulation. Consequently, the problem would need to be solved in several phases when using GPOPS to expedite the computation time. However, since the non-pulsatile and pulsatile models are interchangeable, the optimal control solutions using the non-pulsatile model can be utilized within the pulsatile model to predict R_{aup} and E_m thus eliminating the need for piecewise linear splines and gradient-based optimization.

3 Model validation

Model validations are first done using cycle-averaged pseudo-data extracted from Williams et al. (2014) and second using cycle-averaged HUT data shown in Fig. 2. The first set of model validation was performed to validate the approach of optimal control formulation to predict time-varying quantities controlled by the baroreflex system: Systemic vascular resistance and minimum ventricular elastance. The second model validation is to show the potential of the method for the analysis of clinical data.

3.1 Validation using pseudo-data

As mentioned in Sect. 2.2, pseudo-data were extracted from piecewise linear spline (PWLS) model in Williams et al. (2014). From this study we extracted controlled quantities (vascular resistance and minimum elastance) as well as predicted states including pressures in the four arterial and venous compartments (p_{au}, p_{vu}, p_{al}, and p_{vl} (see Fig. 1)) and cardiac output (CO). Using the objective function (18) we predicted controlled quantities: vascular resistance R_{aup} and minimum elastance E_m using the piecewise linear spline approach discussed in Williams et al. (2014) and using optimal control via GPOPS. Results from simulation for Subject 1 are shown in Fig. 3. For all predictions magenta lines show results obtained using the PWLS model, while cyan lines show predictions from GPOPS. The figure shows dynamics of model states p_{au}, p_{vu}, p_{al}, p_{vl}, CO, V_{tot} and controlled quantities R_{aup} and E_m. Predictions agree well, the goodness of fit are shown on each graph. Though it should be noted that the pseudo-data extracted were all predicted using PWLS predictions of R_{aup} and E_m, and by adapting the control to predict these results may introduce bias, since biologically,

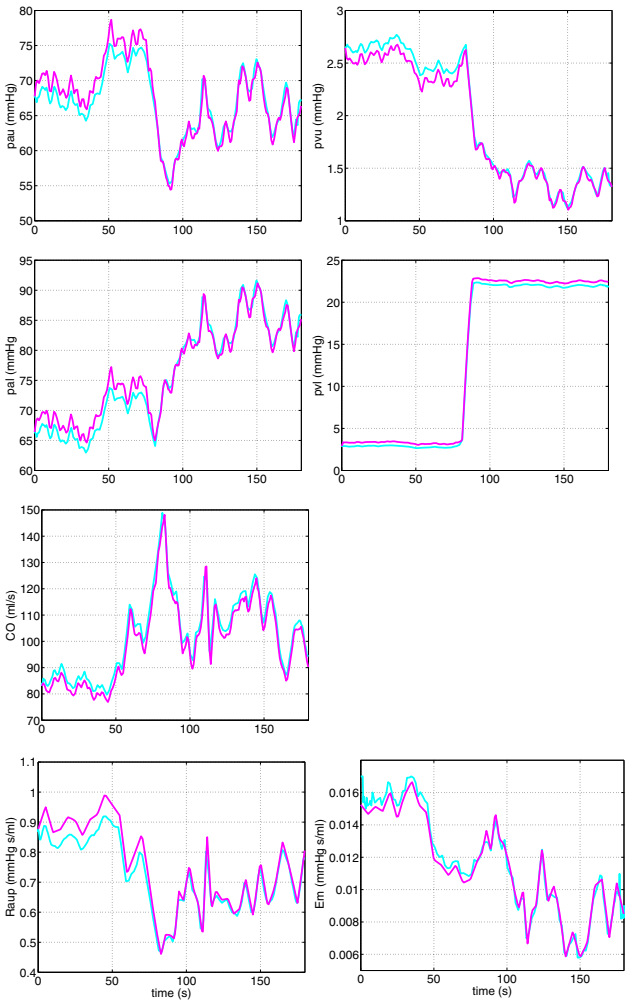

Fig. 3 Predictions during HUT with cost function (18) for Subject 4. All graphs include the non-pulsatile model output, with cardiovascular regulation using the piecewise linear spline method (magenta) and the optimal control method (cyan), for upper body arterial pressure, p_{au}, upper body venous pressure p_{vu}, lower body arterial pressure p_{al}, lower body venous pressure p_{vl}, and cardiac output CO. Also shown are the control variables, upper body peripheral resistance (R_{aup}) and left heart minimum elastance (E_{m}) computed from the optimal control approach via GPOPS (cyan) compared against the piecewise linear spline approach (magenta) in the non-pulsatile model

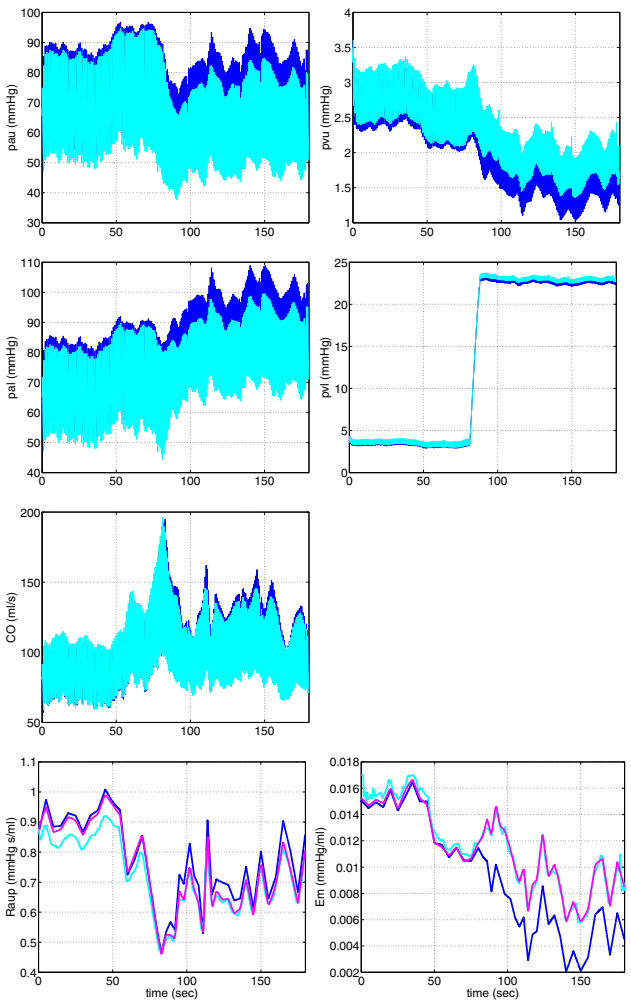

Fig. 4 Pulsatile predictions for Subject 4 during HUT with controlled variables R_{aup} and E_{m} predicted using GPOPS (cyan) and piecewise linear splines (magenta). These predictions are compared with piecewise linear spline estimates obtained from optimizing the cost function (18) using the pulsatile model. Predicted quantities R_{aup} and E_{m} are shown along with predictions of the upper body arterial pressure, p_{au}, the upper body venous pressure p_{vu}, the lower body arterial pressure p_{al}, the lower body venous pressure p_{vl}, and cardiac output CO

the parameters vary nonlinearly, rather than linearly (Smith and Kampine 1990).

Second, we wanted to test predictions from the non-pulsatile models (piecewise linear splines and GPOPS) against those obtained using the pulsatile model. Results of these simulations are shown in Fig. 4. Given that predictions from the non-pulsatile model were almost identical independent of using piecewise linear splines and GPOPS (magenta and cyan lines on Fig. 3), we only show pulsatile predictions comparing GPOPS (cyan) and the pulsatile model (blue). It should be noted that while predictions of upper body vascular resistance R_{aup} is almost identical for the two models, predictions of the minimum elastance E_{m} differ. Predictions with the pulsatile model are lower than those obtained with GPOPS. As a result we see a shift in pressures, though cardiac output is not affected significantly. This is likely a consequence of the fact that the compartment model for the heart is different between the non-pulsatile and pulsatile models. The use of the Frank–Starling mechanism in the non-pulsatile model involves a cardiac contractility parameter S that is not present in the pulsatile model. Even with the slight shift, the change in minimum elastance is similar for the two models.

It should be emphasized that the computational time needed to estimate controlled quantities using piecewise linear spines in the pulsatile model was about three times longer than using GPOPS with the non-pulsatile model.

3.2 Validation using clinical data

In this section, we present results combining the non-pulsatile model with data that can be measured clinically, including arterial blood pressure (measured) and heart rate (synthetic) (shown in Fig. 2) to predict the controlled quantities: vascular resistance R_{aup} and minimum elastance E_{m}. To do so, we employ the objective function

$$J = \int_{t_0}^{t_f} 10^2 \left[\left(\frac{p_{\text{au}}^m - p_{cd}^d}{p_{cd}^d} \right)^2 + \left(\frac{\text{CO}^m - \text{CO}^d}{\text{CO}^d} \right)^2 \right] + R_{\text{aup}}^2 + E_{\text{m}}^2 \, \text{d}t, \tag{19}$$

where p_{cd} is the averaged blood pressure data from each of the five healthy young subjects (black curve in Fig. 2), and CO^d is the synthetically generated cardiac output. Again, the weights in (19) have been determined *a priori* through a series of numerical experiments. Figure 5 depicts results utilizing this cost function and shows data (red) and model predictions (cyan) for the upper body arterial pressure and cardiac output, as well as predictions for R_{aup} and E_{m} with the piecewise linear spline method (magenta) and the GPOPS optimal control method (cyan). Figure 6 shows the predicted control R_{aup} and E_{m} for the 5 subjects via the GPOPS optimal control approach.

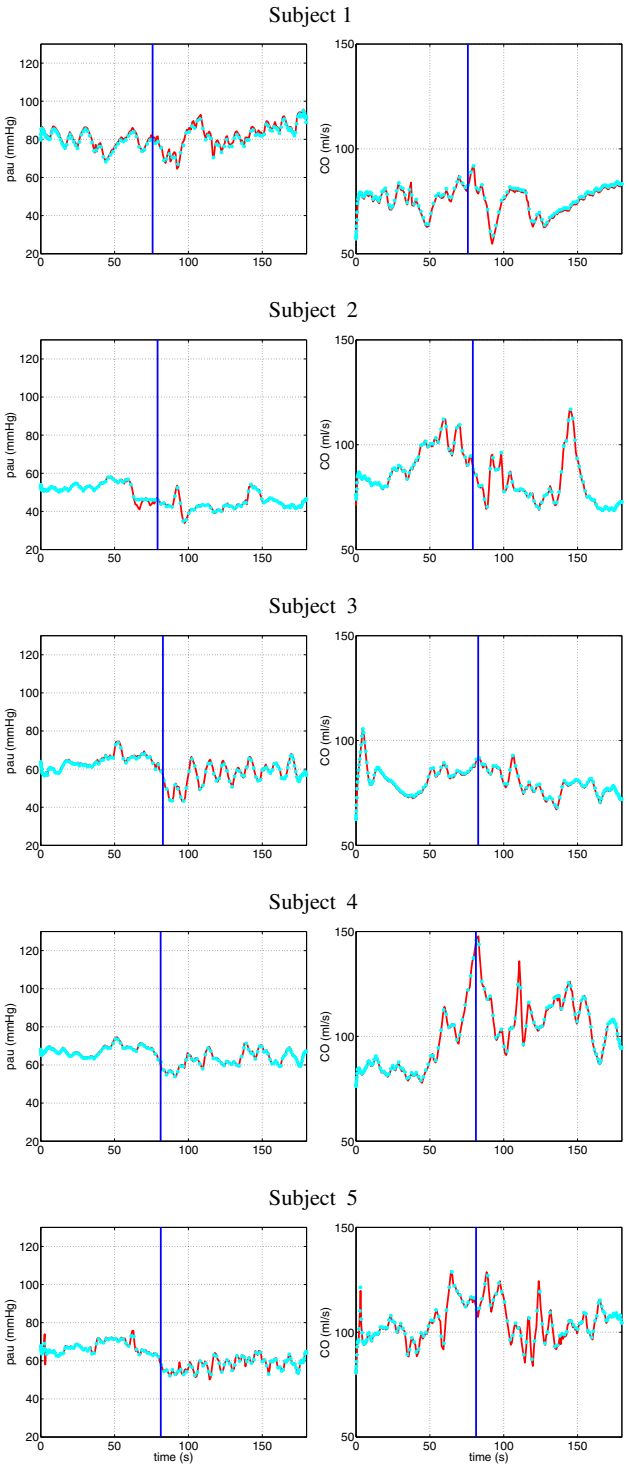

Fig. 5 Predictions during HUT with cost function (19) for all 5 data sets. Graphs shown include data (red) and model predictions via GPOPS (cyan) for upper body arterial pressure p_{au} and cardiac output CO

4 Discussion and conclusions

This study shows that it is feasible to use an optimal control approach to predict time-varying quantities within cardiovascular regulation. The optimal control approach is compared to results from our previous study (Williams et al. 2013; Williams et al. 2014) using a piecewise linear spline approach (summarized in Table 3). Our method proved to be favorable in several ways. First, utilizing the optimal control formulation is advantageous as there is no need to have in depth knowledge of the control variable dynamics before hand. Second, the computation time is significantly reduced with this method. With the optimal control approach, we are able to specify the controlled parameters based on time dependent blood pressure data points in less than triple the amount of time as the piecewise linear spline approach on a Macbook Pro with a 2.66 GHz Intel Core 2 Duo processor. Third, we have also shown that although the optimal control method is suitable for use with a non-pulsatile model, results can be embedded in a pulsatile model rendering accurate dynamics. Optimal control methods have predominately been used in mathematical models of cancer or HIV treatments (David 2007; Pillis and Radunskaya 2003; Neilan and Lenhart 2010; Zarei et al. 2010). The use of optimal control to regulate time-varying quantities to study the control of the cardiovascular system is a novel approach. To our knowledge, Batzel et al. (2007) are the only researchers to have used optimal control to study cardiovascular dynamics. However, they use the method in a very different manner than what we have

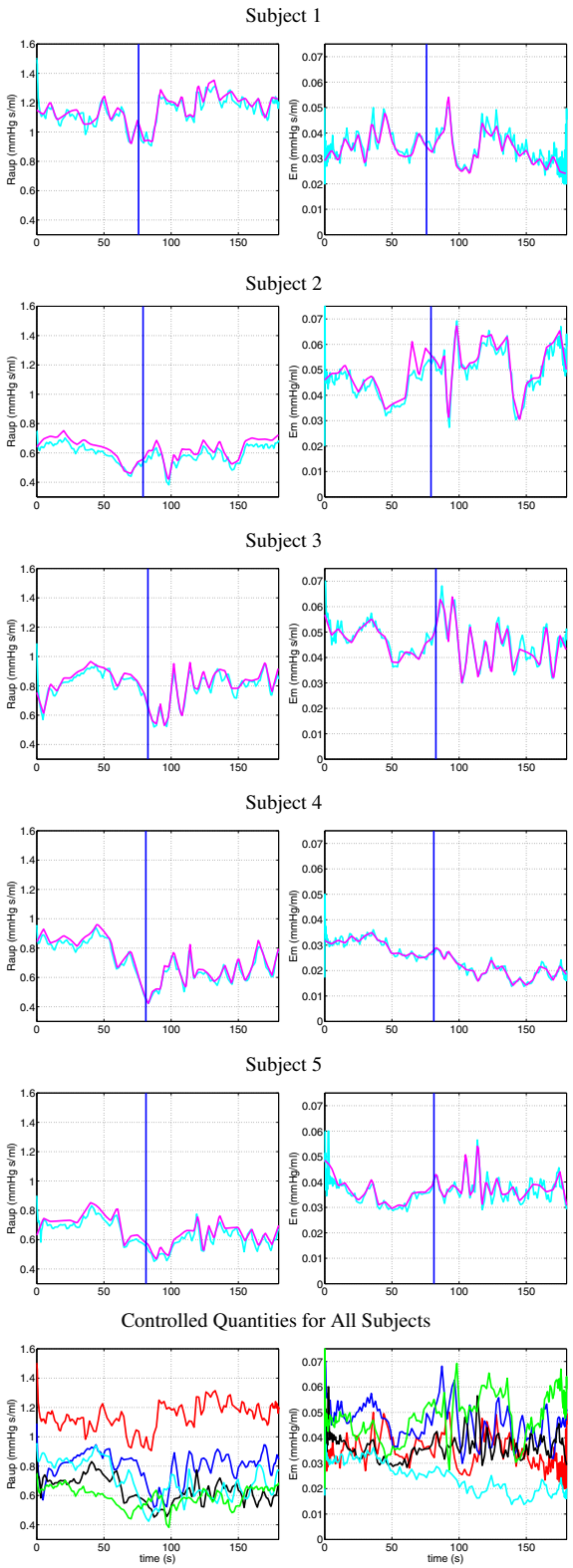

Fig. 6 Upper body peripheral resistance R_{aup} and minimum elastabce E_{m} computed from the optimal control approach via GPOPS (cyan) compared against the piecewise linear spline approach (magenta) using the non-pulsatile model. Also shown are the control variables R_{aup} and E_{m} for all 5 data sets predicted from the optimal control method where each color corresponds to a different subject

Table 3 Comparison of piecewise linear spline (PWLS) and optimal control methods

PWLS	Optimal control
A priori knowledge of control variable dynamics needed	No in depth knowledge of control variable dynamics required
Computationally expensive	Quick simulation time
Implemented with pulsatile and non-pulsatile models	Implemented with non-pulsatile model only

proposed. Here we compared results to a piecewise linear spline approach, other options would have been to compare predictions to Kalman filtering, e.g., used in our previous study (Matzuka et al. 2015) predicting the same parameters using a pulsatile model.

Figures 3 and 5 validate that predicting R_{aup} and E_{m} with an optimal control approach using GPOPS can render almost equivalent dynamics for HUT, compared to using a piecewise linear spline approach coupled with gradient-based optimization. As discussed, the quick timescale of the pulsatile model depicting beat-to-beat dynamics is incompatible with the slower control variables modeling dynamics over an average heart beat within the optimal control approach. However, Fig. 4 illustrates that it is feasible to use optimal control with a simple non-pulsatile model to analyze dynamics for a more complex pulsatile model and yield accurate dynamics.

It is important to note that cardiac output data is essential to ensure accurate model dynamics during HUT as discussed in Williams et al. (2014). To ensure accurate cardiac output estimates it is necessary to either include measurements of cardiac output in the cost function or to predict cardiac output from the blood pressure measurements as proposed in Wesseling et al. (1993) and Parklikar et al. (2007). We have used pseudo-data for CO in our predictions via the previous pulsatile model, however clinicians are able to obtain actual CO data which we will be pursuing in future work. It should be noted that previous simulations were performed under the assumption that CO is constant, yet there are evidence that it may fall during HUT (Zaidi et al. 2000; Zhang et al. 2016). Furthermore, in the future, it would be interesting to see what other data (e.g., venous upper or lower body pressure) can be included to yield improved prediction of the time-varying quantities. A preliminary analysis of this has been done by considering various components in the tilt cost function and observing the results when input into the pulsatile model.

Figures 5 and 6 show results without using the pulsatile model. These plots depict that the optimal control method has the ability to predict forward simulations without having to use a more complex model. The significance of this is now we have the option to analyze longer timescales for both models,

thus enabling us to better understand the cardiovascular system during the entire tilting procedure, including tilting back down to supine position. Moreover, being able to explore longer timescales allows the model to be coupled with larger and more complex systems such as the respiratory or renal systems, which function at timescales of minute–hours rather than seconds–minutes (Levick 2010).

Note that any discrepancy between model predictions involving the pulsatile model and GPOPS may arise due to the fact that GPOPS is utilized with the non-pulsatile model which differs from the pulsatile when modeling the heart compartment. The use of the Frank–Starling mechanism within the non-pulsatile model involves a cardiac contractility parameter S that is not present with the pulsatile model. The coupling of the parameter S and E_{m} together as in (13) causes a variation in predictions of the controlled quantities. Thus, causing variations in the outputs between the pulsatile model with piecewise linear splines and the pulsatile model with the GPOPS predictions. This is one limitation to our model. See Chapter 7 of Williams et al. (2014) for a more in depth explanation. Another limitation to this work is the sensitivity to the upper and lower bounds on quantities needed to utilize GPOPS. A value for a specific parameter or state bound is chosen for biological reasons, however numerically that value may disrupt the calculation of the solution to the optimal control problem, in turn leading GPOPS to be unable to find an optimal solution for the problem or causing the simulation time to increase. Thus, it is important to understand the dynamics of the system and find a balance between the biological significance and the numerical computation.

Compliance with ethical standards

Funding Williams and Olufsen were supported in part by the virtual rat physiology project under grant NIH-NIGMS #1P50GM094503. Tran and Olufsen were supported by NSF under the grant NSF/DMS #1022688. Tran was also supported in part by NIAID under grant NIAID 9R01AI071915. Williams was also supported form the Department of Mathematical Sciences of the United States Military Academy at West Point. This research was performed while Williams held an NRC Research Associateship award at the Army Research Lab.

Conflict of interest The authors declare that they have no conflicts of interest.

Ethical approval All applicable international, national, and/or institutional guidelines for the care and use of animals were followed. All procedures performed in studies involving animals were in accordance with the ethical standards of the institution at which the studies were conducted.

Data The datasets generated during and/or analyzed during the current study are available on request from the corresponding author.

References

Batzel JJ, Kappel F, Timischl-Teschl S (2005) A cardiovascular-respiratory control system model including state delay with application to congestive heart failure in humans. J Math Biol 50:293–335

Batzel JJ, Kappel F, Schneditz D, Tran HT (2007) Cardiovascular and respiratory systems: modeling, analysis, and control. SIAM, Philadelphia

Betts JT (1998) Survey of numerical methods for trajectory optimization. J Guid Control Dyn 21:93–207

Burton AC (1972) Physiology and biophysics of the circulation, 2nd edn. Year Book Medical Publishers, Chicago

David JA (2007) Optimal control, estimation, and shape design: analysis and applications. PhD Dissertation, NC State University, Raleigh, NC

De Pillis LG, Radunskaya A (2003) The dynamics of an optimally controlled tumor model: a case study. Math Comput Model 37:1221–1244

Grodins FS (1959) Integrative cardiovascular physiology: a mathematical synthesis of cardiac and blood vessel hemodynamics. Q Rev Biol 34:93–116

Ellwein LM (2008) Cardiovascular and respiratory modeling. PhD Thesis, NC State University, Raleigh, NC

Engelsone A (2006) Direct transcription methods in optimal control: theory and practice. PhD Dissertation, NC State University, Raleigh, NC

Fink M, Batzel JJ, Kappel F (2004) An optimal control approach to modeling the cardiovascular-respiratory system: an application to orthostatic stress. Cardiovasc Eng 4:27–38

Lanier JB, Mote MB, Clay EC (2011) Evaluation and management of orthostatic hypotension. Am Fam Phys 84:527–536

Levick JR (2010) An introduction to cardiovascular physiology, 5th edn. Hodder Arnold Publishers, London

Matzuka B, Mehlsen J, Tran HT, Olufsen MS (2015) Using Kalman filtering to predict time-varying parameters in a model predicting baroreflex regulation during head-up tilt. IEEE Trans Biomed Eng 62:1992–2000

Miller TH, Kruse JE (2005) Evaluation of syncope. Am Fam Phys 72:1492–1500

Murray W, Gill PE, Saunders MA (2002) SNOPT: an SQP algorithm for large-scale constrained optimization. SIAM J Optim 12:979–1006

Mutsaers M, Bachar M, Batzel JJ, Kappel F, Volkwein S (2007) Receding horizon controller for the baroreceptor loop in a model for the cardiovascular system. Cardiovasc Eng 206:14–22

Nagaiah C, Kunisch K, Plank G (2013) Optimal control approach to termination of re-entry waves in cardiac electrophysiology. J Math Biol 67:359–388

Neilan RM, Lenhart S (2010) An Introduction to optimal control with an application in disease modeling. DIMACS Ser Discret Math Theor Comput Sci 75:67–81

Parklikar TA, Heldt T, Ranade GV, Verghese GC (2007) Model-based estimation of cardiac output and total peripheral resistance. Comput Cardiol 34:379–382

Rao AV, Benson DA, Darby CL, Patterson MA, Francolin C, Sanders I, Huntington GT (2010) Algorithm 902: GPOPS, a MATLAB software for solving multiple-phase optimal control problems using the gauss pseudo-spectral method. ASM Trans Math Softw 22:1–39

Rao AV, Benson DA, Huntington GT (2011) User's manual for GPOPS version 5.0 : a MATLAB software for solving multiple-phase optimal control problems using hp-adaptive pseuodpectral methods. http://www.gpops.org

Robertson DW, Low PA, Polinsky RJ (2004) Primer on the autonomic nervous system, 2nd edn. Academic Press, San Diego

Kappel F, Fink M, Batzel JJ (2007) Aspects of control of the cardiovascular-respiratory system during orthostatic stress induced by lower body negative pressure. Math Biosci 206:273–308

Rowell LB (2004) Ideas about control of skeletal and cardiac muscle blood flow (1876–2003): cycles of revision and new vision. J Appl Physiol 97:384–392

Saunders MA, Gill PE, Murray W, Wright MH (1986) User's guide for NPSOL (version 4.0): a FORTRAN package for nonlinear programming. Tech Rep Dept Oper Res, Stanford University

Shoucri RM (1991) Pump function of the heart as an optimal control problem. J Biomed Eng 13:384–390

Smith JJ, Kampine JP (1990) Circulatory physiology-the essential. The Williams & Wilkins Company, Baltimore

Stryk O, von and Burlirsch R (1992) Direct and indirect methods for trajectory optimization. Ann Oper Res 37:357–373

Wesseling KH, Jansen JRC, Settels JJ, Screuder JJ (1993) Computation of aortic flow from pressure in humans using a nonlinear three-element model. J Appl Physiol 74:2566–2573

Williams ND, Tran HT,Olufsen MS (2013) Cardiovascular dynamics during head-up tilt assessed via a pulsatile and non-pulsatile model. Proc 3rd Int conf on simulation and modeling methodologies, technologies and applications, SciTePress, Sci Technol Pub

Williams ND, Wind-Willassen O, Mehlsen J, Ottesen JT, Olufsen MS (2014) REU-Program. Math Med Biol 31:365–392

Zaidi A, Benitez D, Gaydecki PA, Vohra A, Fitzpatrick AP (2000) Haemodynamic effects of increasing angle of head up tilt. Heart 83:181–184

Zarei H, Kamyad AV, Effati S (2010) Multiobjective optimal control of HIV dynamics. Math Prob Eng 568315:29. https://doi.org/10.1155/2010/568315

Zhang J, Critchley LAH, Lee DCW, Shaw KS, Lee SWY (2016) The effect of head up tilting on bioreactance cardiac output and stroke volume readings using suprasternal transcutaneous Doppler as a control in healthy young adults. J Clin Monit Comput 30:519–526